



**HAL**  
open science

## Modelling porous granular aggregates

Rafik Affes, Vincent Topin, Jean-Yves Delenne, Yann Monerie, Farhang Radjai

► **To cite this version:**

Rafik Affes, Vincent Topin, Jean-Yves Delenne, Yann Monerie, Farhang Radjai. Modelling porous granular aggregates. 9th International Workshop on Bifurcation and Degradation in Geomaterials, May 2011, Porquerolles, France. pp.249-255, 10.1007/978-94-007-1421-2\_32 . hal-04712897

**HAL Id: hal-04712897**

**<https://hal.science/hal-04712897v1>**

Submitted on 3 Oct 2024

**HAL** is a multi-disciplinary open access archive for the deposit and dissemination of scientific research documents, whether they are published or not. The documents may come from teaching and research institutions in France or abroad, or from public or private research centers.

L'archive ouverte pluridisciplinaire **HAL**, est destinée au dépôt et à la diffusion de documents scientifiques de niveau recherche, publiés ou non, émanant des établissements d'enseignement et de recherche français ou étrangers, des laboratoires publics ou privés.



Distributed under a Creative Commons Attribution - NonCommercial 4.0 International License

# Modeling Porous Granular Aggregates

R. Affes, V. Topin, J.-Y. Delenne, Y. Monerie, and F. Radjai

**Abstract** We rely on 3D simulations based on the Lattice Element Method (LEM) to analyze the failure of porous granular aggregates under tensile loading. We investigate crack growth by considering the number of broken bonds in the particle phase as a function of the matrix volume fraction and particle-matrix adhesion. Three regimes are evidenced, corresponding to no particle damage, particle abrasion and particle fragmentation, respectively. We also show that the probability density of strong stresses falls off exponentially at high particle volume fractions where a percolating network of jammed particles occurs. Decreasing the matrix volume fraction leads to increasingly broader stress distribution and hence a higher stress concentration. Our findings are in agreement with 2D results previously reported in the literature.

**Keywords** Damage • Stress transmission • Rheology • Cemented granular materials • Lattice element method

## 1 Introduction

Dense granular materials are characterized either in terms of the network of solid particles or by the properties of the pore space which can be fully or partially filled by a solid binding matrix or a liquid. At high particle volume fractions  $\rho^p$  (typically, for  $\rho^p > 0.57$ ), the stress transmission is basically guided by a

---

R. Affes (✉) · J.-Y. Delenne · F. Radjai  
LMGC, CNRS-Université Montpellier II, Place Eugène Bataillon, 34095 Montpellier Cedex,  
France and Laboratoire MIST, IRSN-CNRS-Université Montpellier 2, Montpellier, France  
e-mail: jean-yves.delenne@univ-montp2.fr; radjai@lmgc.univ-montp2.fr

V. Topin · Y. Monerie  
IRSN, DPAM, CE Cadarache, Bat. 702, 13115 St. Paul-lez-Durance Cedex, France and  
Laboratoire MIST, IRSN-CNRS-Université Montpellier 2, Montpellier, France

percolating network of inter-particle contacts (Satake and Jenkins 1988). This role of the contact network in force transmission and rheological behavior has been mainly investigated in granular materials in the absence of a binding matrix and under compressive confining stresses (Mueth et al. 1998; Radjaï et al. 1996).

The issue of stress concentration and the role of particles are much less evident in the presence of a binding matrix and under tensile loading. Such *porous granular aggregates* have been recently studied in some detail in a 2D geometry by means of numerical simulations (Van Mier et al. 2002; Topin et al. 2007). The overall stiffness and tensile strength of these materials are dependent on the matrix volume fraction  $\rho^m$ , particle volume fraction  $\rho^p$  and particle-matrix adhesion  $\sigma^{pm}$ .

In this paper, we introduce the lattice element method (LEM) in a 3D geometry for the simulation of porous granular aggregates of spherical particles with a solid matrix. Based on a lattice discretization of both phases and their interface as well as an efficient quasi-static time-stepping scheme, the LEM algorithm allows us to analyze the fracture of cohesive aggregates as a function of phase volume fractions and local binding strength.

## 2 Lattice Element Method

The *lattice element method* (LEM) has been recently employed as an alternative to the finite element method for the investigation of the fracture properties of granular materials mixed with a binding matrix (Van Mier et al. 2002; Topin et al. 2007). Such materials, to which we refer in this paper as porous granular aggregates or cemented granular materials can be found in very different forms in nature and industry. Well-known examples are conglomerates and concrete.

In LEM, the space is discretized as a regular or disordered grid of points (nodes) interconnected by one-dimensional elements (bonds). Each bond can transfer normal force, shear force and bending moment up to a threshold in force or energy. Various rheological behaviors can be carried by these material lattice bonds, in contrast to the finite element approach where the local behavior is carried by volume elements. When several phases are present as in a porous granular aggregates, each phase and its boundaries are materialized by lattice elements sharing the same properties and belonging to the same portion of space. We use linear elastic-brittle elements, each element characterized by a Hooke constant and a breaking force threshold. The bonds transmit only normal forces between the lattice nodes and thus the strength of the lattice in shear and distortion is ensured only by the high connectivity of the nodes. This simple kinematics allows to investigate high sampling statistical approach. A sample is defined by its contour and the configuration of the phases in space. The samples are deformed by imposing displacements or forces to nodes belonging to the contour. The initial state is the reference (unstressed) configuration. The total elastic energy of the system is a convex function of node displacements and thus finding the unique equilibrium configuration of the nodes amounts to a minimization problem (implemented here

by means of the conjugate gradient method). Performing this minimization for stepwise loading corresponds to subjecting the system to a quasi-static deformation process. The overloaded elements (exceeding a threshold) are removed according to a breaking rule. This corresponds to irreversible micro-cracking of the lattice. The released elastic energy between two successive equilibrium states is thus fully dissipated by micro-cracking. In the fast implementation used in the present work, all overloaded elements occurring within the same step are removed, as well as those appearing recursively after energy minimization (within the same step). This corresponds physically to unstable growth of the micro-cracks compared to the imposed strain rate.

The 3D LEM has the advantage to be cheap in computational effort, making it possible to simulate systems with an large number of nodes for reasonable computing time. It should be remarked that due to the simple additivity of the potential energy, the computation time depends only linearly on the number of nodes. It is also obvious that the LEM is a convenient model of brittle fracture in which the generation and propagation of cracks are “naturally” taken into account.

### 3 Application to Granular Aggregates

In a granular aggregate, there are three bulk phases: particles, matrix and voids. There are also two interface phases: particle–particle and particle–matrix; see Fig. 1. To construct the samples, we first generate a large dense packing of rigid spherical particles compressed isotropically by means of the contact dynamics method. A cubic portion of this three-dimensional packing is overlaid on a disordered tetrahedral lattice. The particle properties are attributed to the bonds falling in the bulk of the particle phase. The binding matrix is then added in the form of bridges of variable width connecting neighboring particles within a prescribed gap between

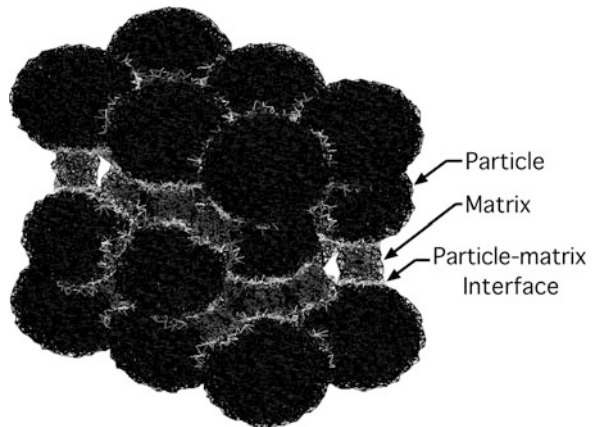
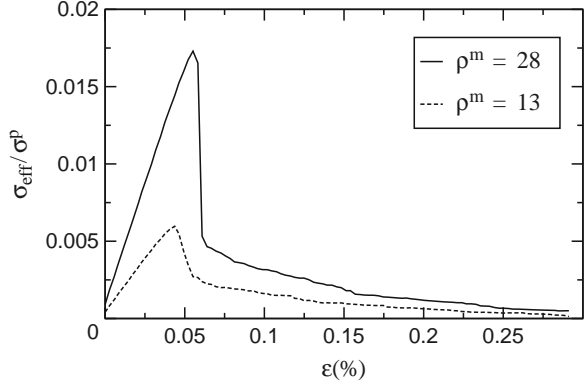


**Fig. 1** Example of a discretized aggregate involving particles, matrix, voids and particle–particle and particle–matrix interface zones

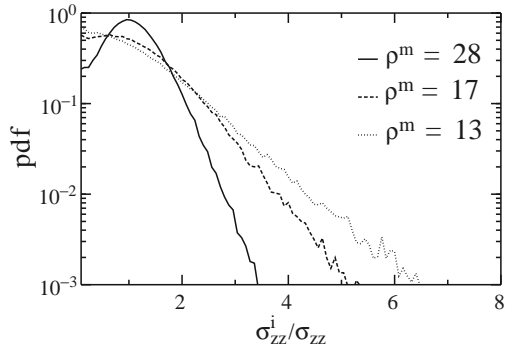
particles. The bonds belonging to these bridges are given the properties of the matrix. In the same way, the bonds falling between a particle and the matrix or between two particles are given the properties of the corresponding interface. The width of solid bridges between particles is proportional to the total volume of the binding material. At higher levels of the matrix volume fraction, the bridges overlap and the porosity declines to zero. The particles are polydisperse with diameters varying nearly uniformly in size in a range  $[0.8d, d]$ . The total particle volume fraction is about 0.6 corresponding to a dense close packing. The samples consist of the bulk phases: (1) particles, denoted  $p$ ; (2) matrix, denoted  $m$ ; and (3) void space or pores, denoted  $v$ , as well as the interface phases: (1) particle–particle interface, denoted  $pp$ , and (2) particle–matrix interface, denoted  $pm$ . The elements belonging to each phase  $\phi$  (bulk or interface) are given a Hooke constant  $k^\phi$  and a breaking force  $f^\phi$ . We have  $f^v = 0$  and the choice of the value of  $k^v$  is immaterial. The interface phases  $pm$  and  $pp$  are transition zones of finite width. But for large systems, the volume fractions of these transition zones are negligible compared to those of the particles and matrix. The interface phases affect the global behavior through their specific surface and their strengths represented by the Hooke constants  $k^{pp}$  and  $k^{pm}$  and the corresponding tensile force thresholds  $f^{pp}$  and  $f^{pm}$ . In our simulations, we model the interface phases by a one bond-thick layer linking two particles or a particle to the matrix. The volume fractions of the interface phases are thus assumed to be zero ( $\rho^{pp} = \rho^{pm} = 0$ ) and the volume fractions  $\rho^p$ ,  $\rho^m$  and  $\rho^v$  are attributed only to the three bulk phases, with  $\rho^p + \rho^m + \rho^v = 1$ . It is dimensionally convenient to express the bond characteristics in stress units. We thus define the bond breaking (or debonding) stresses  $\sigma^\phi = \frac{f^\phi}{a^2}$  and the moduli  $E^\phi = \frac{k^\phi}{a}$  where  $a$  is the length of the lattice vector. These bond moduli  $E^\phi$  of the lattice should be carefully distinguished from the equivalent phase moduli which depend both on the bond moduli and the geometry of the lattice. We will use below square brackets to represent the phase moduli:  $E^{[p]}$ ,  $E^{[m]}$ ,  $E^{[pp]}$  and  $E^{[pm]}$ . It can be shown that the overall Young modulus and Poisson ratio of an disordered isotropic tetrahedral lattice are  $E^{eff} = \frac{5}{4\sqrt{2}}E^\phi$  and  $\nu^{eff} = 0.25$ . We performed a serie of simple tension tests over samples composed of 516 particles. The particle volume fraction was kept constant  $\rho^p = 0.6$ , and  $\rho^m$  was varied from  $\rho^p/10$  to  $4\rho^p$ . Each sample was discretized over a lattice containing about  $1.5 \times 10^6$  elements. The results presented below were obtained for hard particles  $E^p = 3E^m$ ,  $\sigma^p = \sigma^m$  and  $\sigma^{pp} = 0$ . The cubic samples were subjected to uniaxial tension with free lateral sides. The nodes belonging to the base were constrained to be immobile. Upward step-wise displacements were applied to the nodes belonging to the upper surface.

Figure 2 shows the stress–strain plot under for  $\rho^m = 28\%$  and  $\rho^m = 13\%$ . We observe a brittle behavior with a well-defined initial stiffness  $E_{eff}$  and a tensile strength  $\sigma_{eff}$  at the stress peak. The post-peak behavior is characterized by nonlinear propagation of the main crack (initiated at the stress peak) in the form of a sequence of loading–unloading events. The stiffness declines due to progressive damage of the aggregate. The overall tensile strength is higher at larger  $\rho^m$  as a result of a weaker concentration of stresses. The probability distribution functions

**Fig. 2** Normalized vertical stress as a function of vertical strain in tension for two values of the matrix volume fraction  $\rho^m$  (in %)



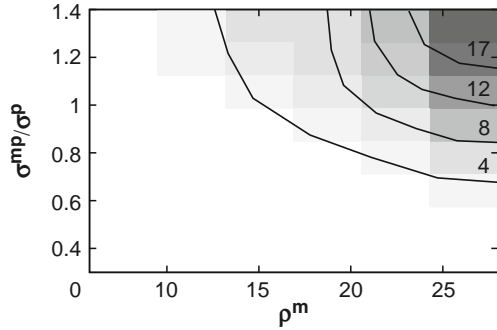
**Fig. 3** Probability densities of normalized vertical node stresses  $\sigma_{zz}^i$  for three values of the matrix volume fraction  $\rho^m$  (in %)



of vertical node stresses  $\sigma_{zz}$  are shown in Fig. 3. From the shapes of the pdf's, we distinguish large stresses falling off exponentially as observed for large contact forces in granular media (Mueth et al. 1998; Radjaï et al. 1996). The weak stresses have nonzero probability (increasing as  $\sigma_{zz} \rightarrow 0$ ) reflecting the arching effect whereas intermediate stresses are centered on the mean and define a nearly Gaussian distribution. The large stresses mostly concentrate at the contact zones and they form well-defined chains that cross the particles.

The tensile strength and crack propagation are controlled by both  $\rho^m$  and  $\sigma^{pm}$ . For a quantitative evaluation of this effect, we consider here the proportion  $n_b$  of broken bonds inside the particles with respect to the total number of broken bonds. Figure 4 shows a map of  $n_b$  in the parameter space  $(\rho^m, \sigma^{pm})$  following failure. We see that below a well-defined frontier, no particle damage occurs ( $n_b \simeq 0$ ). For this range of parameter values, the cracks propagate either in the matrix or at the particle-matrix interface. Above this ‘‘particle-damage’’ limit, the isovalue lines become nearly parallel to the limit line with an increasing level of  $n_b$ . This suggests three distinct regimes of crack propagation: (1) below the particle-damage limit, the cracks bypass the particles and propagate through the matrix, the pores or along the particle-matrix interface; (2) above this limit and for  $\rho^m < 20$ , the cracks penetrate

**Fig. 4** Grey level map of the fraction of broken bonds in the particle phase for different values of matrix volume fraction and particle-matrix adhesion



into the particles from solid bridges that strongly concentrate stresses; (3) Above this limit, the cracks propagate inside the matrix as well as across the particles, causing the *fragmentation* of the particles. These results are qualitatively similar in 2D cohesive granular aggregates (Topin et al. 2007).

## 4 Conclusion

In this paper, a lattice-based discretization approach (lattice element method) was introduced and illustrated by application to the brittle failure of porous granular aggregates. In contrast to dilute particle-reinforced composites, such materials involve a high level of particle volume fraction and thus a jammed skeleton of solid particles interconnected via a binding matrix. The overall behavior depends on the bulk phase volume fractions and the properties of the particle–particle and particle-matrix interface zones. We found that the presence of the particle skeleton controls stress concentration and thus the strength properties of these materials. It was also shown that for a range of the values of the particle-matrix adhesion and matrix volume fraction, no particle damage occurs. The trends are very similar to those previously established for 2D aggregates by the same model.

## References

- D.M. Mueth, H.M. Jaeger, S.R. Nagel, Force distribution in a granular medium. *Phys. Rev. E*. **57**, 3164 (1998)
- F. Radjaï, M. Jean, J.-J. Moreau, S. Roux, Force distribution in dense two-dimensional granular systems. *Phys. Rev. Lett.* **77**(2), 274 (1996)
- M. Satake, J.T. Jenkins, *Micromechanics of Granular Materials* (Elsevier, Amsterdam, 1988)
- V. Topin, J.-Y. Delenne, F. Radjaï, L. Brendel, F. Mabilbe, Strength and fracture of cemented granular matter. *Eur. Phys. J. E. Soft Matter*. **23**, 413–429 (2007)
- J.G.M. Van Mier, M.R.A. Van Vliet, T.K. Wang, Fracture mechanisms in particle composites: statistical aspects in lattice type analysis. *Mech. Mater.* **34**(11), 705–724 (2002)